Magnetic-field decoupling of an alkali-metal excited-state hyperfine structure

W. A. van Wijngaarden and J. Sagle
Department of Physics, York University, Toronto, Ontario, Canada M3J 1P3
(Received 27 July 1990)

The theory of how excited-state hyperfine structure can be determined using a magnetic field to decouple the nuclear and electronic angular momentum is presented. The initial excited state is assumed to have an anisotropic Zeeman sublevel population distribution, which can be conveniently created by a laser-induced multiphoton excitation of an unpolarized atom. The Zeeman sublevel populations are subsequently mixed by the hyperfine interaction. The degree of mixing is controlled by a magnetic field applied along the quantization axis. The relative Zeeman sublevel populations can be monitored by detecting the polarization of fluorescence emitted when the excited state radiatively decays. It is convenient to take the ratio of two time-integrated fluorescent signals measured for orthogonal linear polarizations, since this is independent of the excited-state number density. The plot of this ratio versus magnetic field is very well approximated by a Lorentzian curve whose half-width is proportional to the magnetic dipole hyperfine coupling constant. This method was used to determine the magnitude of the magnetic dipole constant of the cesium $8D_{3/2}$ state to be 3.92±0.10 MHz, which is in excellent agreement with previous results.

I. INTRODUCTION

The hyperfine structure of the lowest alkali-metal excited states has been investigated using lamps and continuous-wave lasers to excite the ground state. To populate higher states, stepwise excitation[1] or multiphoton excitation using pulsed lasers is required.[2] The work to date has focused on measuring the hyperfine structure of the lower excited states as is discussed in the review paper of Arimondo *et al.*[3] In this paper, we show how the hyperfine structure of excited states populated by a multiphoton excitation of the ground state can be determined using a magnetic field to decouple the nuclear and electronic angular momenta.

The apparatus is schematically shown in Fig. 1. A laser pulse, linearly polarized along the quantization direction z, populates an excited state. Hence, only Zeeman sublevels obeying the selection rule $\Delta m = 0$ are populated. This is illustrated in Fig. 2(a) where an atom having an $S_{1/2}$ ground state is excited via a two-photon excitation to a $D_{3/2}$ state. The Zeeman sublevels are not eigenstates of the hyperfine Hamiltonian. The hyperfine interaction mixes the sublevel populations as shown in Fig. 2(b). The amount of mixing depends on the strength of the hyperfine interaction and the size of the magnetic field applied along the z direction. The magnetic field decouples the nuclear and electronic spins, thereby hindering the transfer of atoms among the excited-state sublevels. The relative populations of the Zeeman sublevels can be monitored by detecting the fluorescence polarization when the excited state e radiatively decays to a lower state f. In our experiment, this time decaying fluorescence is detected and integrated by a boxcar integrator. It is convenient to simultaneously monitor two fluorescence channels sensitive to orthogonal polarizations since the ratio of these two signals is independent of the excited-state number density. A computer then plots the ratio of the integrated fluorescence intensities versus the magnetic field. This so-called decoupling curve can be very closely approximated by a Lorentzian curve, having a magnetic-field half-width proportional to the magnitude of the hyperfine interaction.

In this paper, we shall first give a detailed presentation of the theory for the general case where the states e and f have arbitrary angular momentum. We considered the case where the electric quadrupole hyperfine interaction is negligible compared to the magnetic dipole interaction.

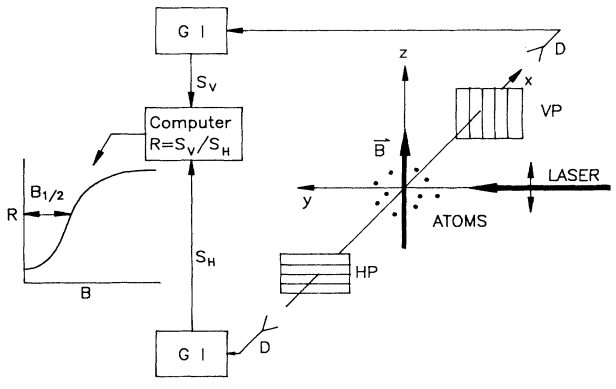

FIG. 1. Schematic experimental arrangement: The atoms are excited by a laser polarized along the z or vertical direction. Vertical (VP) and horizontal (HP) polarized fluorescence are detected by two detectors (D). The fluorescent signals are sent to gated integrators (GI) whose outputs are in turn input to a computer. The computer determines the ratio of the two signals S_V and S_H, and plots it as a function of the magnetic field B.

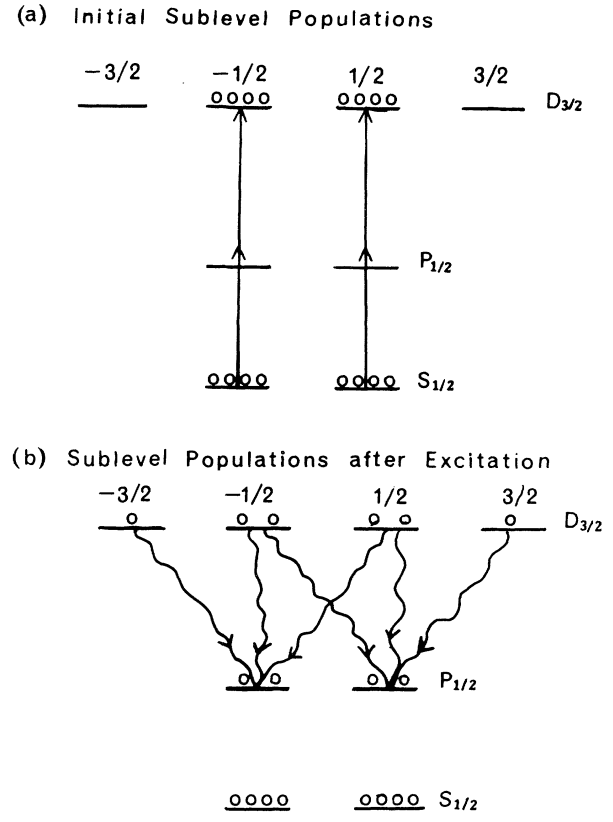

FIG. 2. Zeeman sublevel populations during experiment: (a) illustrates the population of the $m_J=\pm 1/2$ sublevels of the $D_{3/2}$ state produced by a two-photon excitation of the ground state. In (b), the atoms have been redistributed among the sublevels as a result of the hyperfine interaction and fluorescent decay to lower states such as $P_{1/2}$.

The electric quadrupole moment is zero for nuclei having spin less than one and is known to be small for other nuclei such as ^{133}Cs which has spin 7/2.[4] Section III describes a decoupling experiment which determined the magnetic dipole hyperfine constant of the cesium $8D_{3/2}$ state. Finally, Sec. IV compares this result to those found with level crossing and quantum-beat experiments.

II. THEORY

We shall consider an excited state e having angular momentum J_e. This state is populated by a laser, which is linearly polarized along the quantization direction z, at time $t=0$. The populations of the excited-state Zeeman sublevels, labeled by azimuthal quantum number m_J, are assumed to be given by the following:

$$\langle J_e m_J|\rho_e(0)|J_e m_J\rangle = C + D m_J^2 \ . \tag{1}$$

Here $\rho_e(0)$ is the initial excited-state density matrix while C and D are constants satisfying the normalization condition $\mathrm{Tr}\rho_e(0)=1$. We also assume that $\rho_e(0)$ has no off-diagonal matrix elements between the basis states $|J_e m_J\rangle$. Such a distribution of purely aligned atoms[5] is created when linearly polarized light excites an unpolarized state. Other initial states can also be generated. For example, circularly polarized light can be used to orient the atoms in the excited state.[6] In this paper, we consider the common case of pure alignment given by (1). The analysis for other initial states proceeds similarly.

We next introduce the irreducible tensor operator[7]

$$T_{LM}(J,J') = \sum_m |J_m\rangle\langle J' m-M|(-1)^{m-M-J} \times C(J,J',L;m,M-m) \tag{2}$$

where the bra and ket vectors are understood to be quantized along the z axis and C is a Clebsch-Gordan coefficient. The initial excited-state density matrix can then be rewritten as follows:

$$\rho_e(0) = [A_0 T_{00}(J_e,J_e) + A_2 T_{20}(J_e,J_e)] T_{00}(I,I) \tag{3}$$

where A_0 and A_2 are linear combinations of the constants C and D. In writing (3), we have added the operator $T_{00}(I,I)$ since the nucleus of spin I is assumed to be unpolarized. Equation (3) expresses the initial density matrix in terms of the basis set $\{|Jm_J Im_I\rangle\}$. An alternate basis set is $\{|JIFm_F\rangle\}$ where $\mathbf{F}=\mathbf{J}+\mathbf{I}$ is the sum of the electronic and nuclear angular momentum and m_F is the azimuthal component of $\mathbf{F}$. The initial density matrix can then be expressed as follows:[8]

$$\rho_e(0) = \frac{1}{[I]^{1/2}} \left[\frac{A_0}{[J_e]^{1/2}} + A_2 \sum_{F,F'} ([F][F'])^{1/2} W(I,F,J_e,2;J_e,F') T_{20}(F,F') \right] \tag{4}$$

where $[I]=2I+1$ is the statistical weight.

The excited-state density matrix at time t is given by

$$\rho_e(t) = e^{-iHt/\hbar} \rho_e(0) e^{iHt/\hbar} e^{-t/\tau} \tag{5}$$

where τ is the radiative lifetime of state e. The Hamiltonian H is given below:

$$H = H_0 + ah\mathbf{I}\cdot\mathbf{J} + bh \frac{3(\mathbf{I}\cdot\mathbf{J})^2 + \frac{3}{2}(\mathbf{I}\cdot\mathbf{J}) - (\mathbf{I}\cdot\mathbf{I})(\mathbf{J}\cdot\mathbf{J})}{2I(2I-1)J(2J-1)} + g_J\mu_B \mathbf{B}\cdot\mathbf{J} + g_I\mu_N \mathbf{B}\cdot\mathbf{I} \ . \tag{6}$$

H_0 represents the Coulomb and fine structure. The next two terms are the magnetic dipole and electric quadrupole hyperfine interactions, whose magnitude depends on

the coupling constants a and b. The final two terms describe the interaction of the electron and nucleus with an external magnetic field **B**. μ_B and μ_N are the Bohr and nuclear magnetons, respectively, while g_J and g_I are the Lande g factors corresponding to the electronic angular momentum **J** and nuclear angular momentum **I**. The interaction of the nucleus with an external magnetic field can be ignored at the low fields needed to decouple excited-state hyperfine structure, since $\mu_B \gg \mu_N$. We shall consider the case where the electric quadrupole strength b is negligible. The magnetic-field half-width of the decoupling curve then depends only on the magnetic dipole constant a rather than on a linear combination of the coupling constants a and b.

The effect of the Hamiltonian on the excited state is determined by detecting the fluorescence emitted when the excited state e radiatively decays to state f. The fluorescent power $P(t)$ reaching the detector is given by[9]

$$P(t)=N_e \mathrm{Tr}[\mathcal{L}\rho_e(t)] \tag{7}$$

where N_e is a constant proportional to the excited-state number density, the solid angle of the detector, and the transmission efficiency of various optical filters and polarizers. For the case where the detector is unable to resolve the hyperfine components of the fluorescence, the fluorescent light operator $\mathcal{L}$ is defined by

$$\mathcal{L}=\sum_L (-1)^L W(J_f,J_e,1,L;1,J_e) \times \sum_M (-1)^M \mathsf{U}_{L-M}\cdot \mathsf{T}_{LM}(J_e,J_e) \ . \tag{8}$$

W is a Racah coefficient and the tensor U_{LM} is defined as follows:

$$\mathsf{U}_{LM}=\sum_m u_m (u_m - M)^* (-1)^{m-M-1} C(1,1,L;m,M-m) \ . \tag{9}$$

Here u_m is the spherical vector component of the vector describing the polarization of detected fluorescence. When linearly polarized light is detected, $\hat{u}=(0,\sin\theta,\cos\theta)$ where θ is the angle between the z direction and the polarized axis of the detected fluorescence (i.e., $\theta=0$ for vertically polarized light and $\theta=\pi/2$ for horizontally polarized light). The only nonzero U_{LM} then are the following:

$$\begin{aligned} \mathsf{U}_{00}&=\frac{1}{\sqrt{3}} \ , \\ \mathsf{U}_{2\pm 2}&=\frac{\sin^2\theta}{2} \ , \\ \mathsf{U}_{2\pm 1}&=i\cos\theta\sin\theta \ , \\ \mathsf{U}_{20}&=\frac{1}{\sqrt{6}}(1-3\cos^2\theta) \ . \end{aligned} \tag{10}$$

To compute the fluorescent intensity, we need to evaluate matrix elements of $\rho_e(t)$ and $\mathcal{L}$. This must in general be done numerically, since no convenient basis of eigenstates exists that simultaneously diagonalizes the hyperfine and magnetic-field interaction terms of the Hamiltonian. Using the basis set of eigenstates $\{|i\rangle\}$ such that $H|i\rangle=E_i|i\rangle$, the expression for fluorescent power becomes

$$P(t)=N_e \sum_{i,j} \langle i|\mathcal{L}|j\rangle\langle j|\rho_e(t)|i\rangle \ . \tag{11}$$

Using (5), one finds

$$P(t)=N_e e^{-t/\tau}\sum_{i,j} e^{i\omega_{ij}t}\langle i|\mathcal{L}|j\rangle\langle j|\rho_e(0)|i\rangle \tag{12}$$

where $\hbar\omega_{ij}=E_i-E_j$. Integrating the fluorescent power for a time much larger than the radiative lifetime τ, we obtain the signal.

$$S(B,\theta)=\int_0^\infty P(t)dt \ . \tag{13}$$

This integrated fluorescent power has been written as a function of the magnetic-field strength B and the fluorescence polarization angle θ. Next we substitute (11) into (13) and use the symmetry property of the density matrix given in (3) [i.e., $\langle j|\rho_e(0)|i\rangle=\langle i|\rho_e(0)|j\rangle$] to get the following:

$$S(B,\theta)=2\tau N_e \sum_{i,j} \frac{\langle i|\mathcal{L}|j\rangle\langle j|\rho_e(0)|i\rangle}{1+\omega_{ij}^2\tau^2} \ . \tag{14}$$

In practice, it is convenient to compute the ratio of integrated fluorescent powers polarized parallel and perpendicular to the z axis. This ratioed signal given by

$$R(B)=\frac{S(B,0)}{S(B,\pi/2)} \tag{15}$$

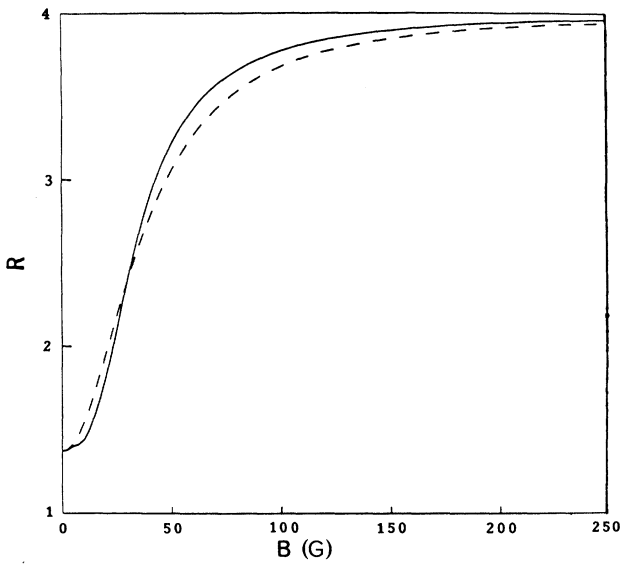

FIG. 3. Lorentzian fit to computed signal ratio: The solid line is the signal ratio R computed for the $D_{3/2}$ state illustrated in Fig. 2. The $D_{3/2}$ state was assumed to have a magnetic dipole constant $a=4.00$ MHz and a radiative lifetime of 150 nsec. The dashed line is a Lorentzian function that was fit to the exact signal as is described in the text.

depends on the lifetime τ, but is independent of the excited-state number density which can be difficult to determine reliably. Figure 3 shows a plot of $R(B)$ that was computed for the case shown in Fig. 2. The $D_{3/2}$ state was specified to have a lifetime of 150 nsec and hyperfine constant $a=4.00$ MHz. At zero magnetic field, the orbital angular momentum **J** and nuclear angular momentum **I** are coupled to produce the vector **F** whose magnitude and component along the z axis are conserved quantum numbers. At strong magnetic fields, **J** and **I** precess about the magnetic field and are completely decoupled from each other. Hence the plot shown in Fig. 3 is called a decoupling curve. We shall show how the magnetic dipole constant is determined from the field half-width of the decoupling curve. Hence it is relatively insensitive to factors affecting the signal amplitude such as the finite solid angle of the detector.

The zero and high field values of the ratio $R(B)$ shall now be evaluated. For the case of zero magnetic field, the eigenstates of the Hamiltonian are $|JIFm_F\rangle$ corresponding to eigenenergy $E_F=(a/2)[F(F+1)-J(J+1)-I(I+1)]$. The integrated fluorescence power is then given by the following:

$$S(0,\theta)=2\tau N_e\left[A_0\frac{U_{00}}{[J_e]^{1/2}}W(J_f,J_e,1,0;1,J_e)+A_2\frac{U_{20}(\theta)}{[I]^{1/2}}W(J_f,J_e,1,2;1,J_e)\times\left[2\sum_{F<F'}\frac{[F][F']W^2(I,F,J_e,2;J_e,F')}{1+\omega_{FF'}^2\tau^2}+\sum_F[F]^2W^2(I,F,J_e,2;J_e,F)\right]\right]. \tag{16}$$

The term summed over F and F' can be neglected in the limiting case of a strong hyperfine interaction defined by $\omega_{FF'}\tau\approx 2\pi a\tau\gg 1$. The quantity $\omega_{FF'}\tau$ is the number of quantum beats occurring in the temporal decay of the fluorescence signal during the lifetime of the excited state. It therefore measures how much the excited-state sublevel populations are mixed by the hyperfine interaction. The condition $2\pi a\tau\gg 1$ is valid for many excited states, and will therefore be assumed to hold in the remainder of this paper. The zero field signal ratio $R(0)$ is then independent of the lifetime τ. This is illustrated in Fig. 4 which shows a plot of $R(0)$ which was computed for atoms excited to the $D_{3/2}$ as shown in Fig. 2.

In the limit where the magnetic field interaction with the electron dominates the Hamiltonian, the eigenstates are $|Jm_J\mathrm{I}m_I\rangle$ corresponding to eigenenergy $E_J=g_J\mu_B Bm_J$. The integrated fluorescence power then becomes

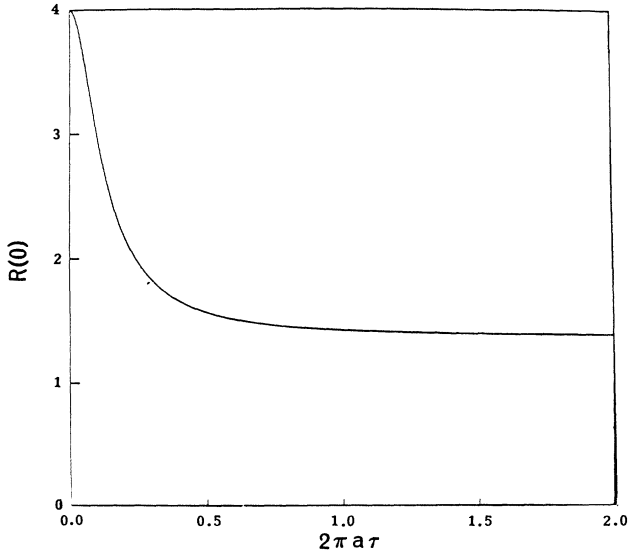

FIG. 4. $R(0)$ is the zero field signal ratio computed for the $D_{3/2}$ state shown in Fig. 2. This graph shows that $R(0)$ is independent of the excited-state lifetime τ when $2\pi a\tau\gg 1$.

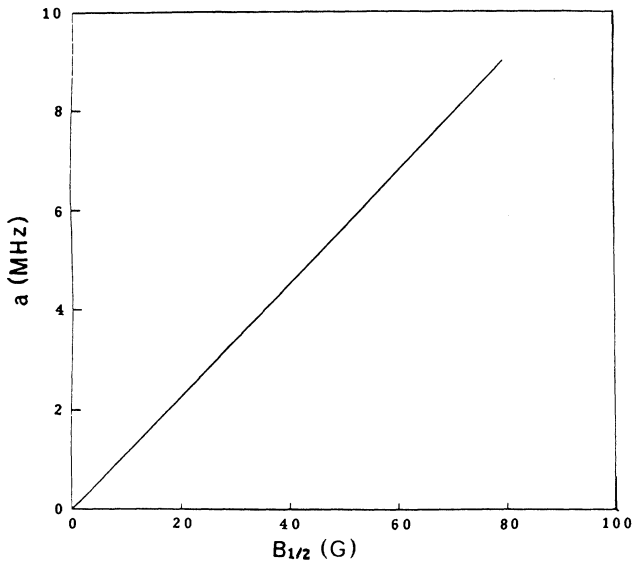

FIG. 5. Plot of magnetic dipole hyperfine constant a vs magnetic-field half-width $B_{1/2}$: The half-widths of decoupling curves such as shown in Fig. 3 were computed and are plotted above. The decoupling curves were found for atoms initially excited in the $D_{3/2}$ state shown in Fig. 2.

$$S(B,\theta)=2\tau N_e\left[A_0\frac{U_{00}}{[J_e]^{1/2}}W(J_f,J_e,1,0;1,J_e)\right.$$
$$\left.+A_2U_{20}(\theta)W(J_f,J_e,1,2;1,J_e)\right]. \quad (17)$$

The high field signal ratio $R(B)$ is then independent of the excited-state lifetime τ. Hence the decoupling curve is completely independent of the excited-state lifetime when $2\pi a\tau \gg 1$.

It is useful to define a parameter $B_{1/2}$ which is the field where the ratioed signal given by (15) is halfway between the zero and high field values denoted by $R(0)$ and $R(B_\infty)$, respectively; i.e.,

$$R(B_{1/2})=\frac{R(0)+R(B_\infty)}{2}. \quad (18)$$

The exact signal can be approximated by a Lorentzian function as is shown in Fig. 3. The Lorentzian curve was chosen to have the same half-width as determined by (18) for the exact signal, and to have zero and high field values found by substituting Eqs. (16) and (17) in (15). Given the very close agreement between the exact signal and the fitted curve, data analysis can be expedited by fitting a Lorentzian function to the experimentally measured data points. We estimate the error in equating $B_{1/2}$ to the half-width at half maximum (HWHM) of the Lorentzian curve to be a few percent.

The magnetic-field half-width $B_{1/2}$ resulting from a given magnetic dipole constant a can be numerically computed using (18). Figure 5 shows a plot of a versus $B_{1/2}$ computed for atoms excited to the $D_{3/2}$ state shown in Fig. 2. The magnetic dipole constant corresponding to an experimentally determined field half-width is found from this graph.

III. EXPERIMENT

A. Apparatus and procedure

A diagram of the apparatus is shown in Fig. 6. A frequency doubled Nd:YAG (where YAG denotes yttrium aluminum garnet) laser pumped a dye laser at a 10 Hz repetition rate. The dye laser was tuned to 7191 Å to excite the cesium $6S_{1/2}$ ground state to the $8D_{3/2}$ state via a two-photon excitation. The laser was linearly polarized along the the vertical or z axis.

The cesium atoms were contained in a cylindrical Pyrex cell having a length of 10 in. and a diameter of 1 in. Before the cell was filled with cesium, it was simultaneously evacuated by a diffusion pump and baked overnight at several hundred degrees centigrade to remove impurities. The cesium cell was located in an oven heated by jets of hot air. A feedback circuit stabilized the temperature to ± 0.1 °C.

Fluorescent light was detected in the direction perpendicular to both the laser propagation and polarization directions as shown in Fig. 6. The detected light first

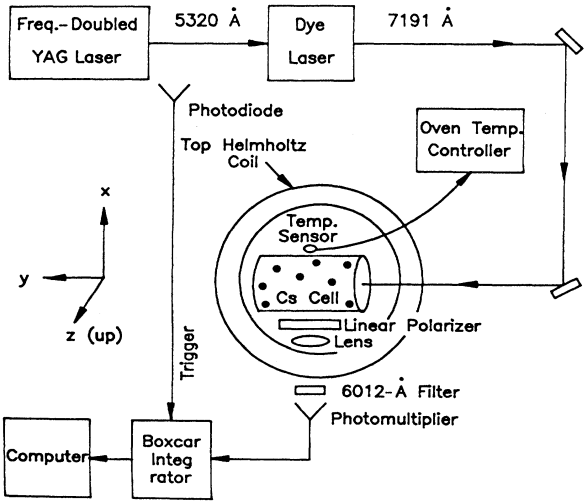

FIG. 6. A diagram of the apparatus.

passed through a linear polarizer whose transmission axis was along either the vertical ($\theta=0$) or horizontal direction ($\theta=\pi/2$). The light was next collimated by a lens onto an interference filter. The filter had maximum transmission at 6012 Å which is the wavelength of light emitted when the cesium $8D_{3/2}$ state radiatively decays to the $6P_{1/2}$ level. The full width at half maximum (FWHM) bandwidth of the filter was only 10 Å. Finally, the light was focused onto a photomultiplier (Hamamatsu model R928). The photomultiplier was located in a mu-metal housing to shield it from magnetic fields. It was operated at sufficiently low voltages to avoid saturation. The time decaying electronic photomultiplier signal was sent to a boxcar which integrated the signal over several lifetimes. The boxcar (Stanford Research Systems 250) was triggered by a fast photodiode that detects the output of the YAG laser. The output of the boxcar was then sent to a computer.

We alternately detected vertical and horizontal polarized fluorescence as follows. The computer averaged the boxcar signals for typically 300 laser shots. The linear polarizer orientation was then switched and the measurement was repeated. The computer then calculated the ratio of the two averaged signals and stored it as a function of the magnetic field. (Ideally, two detectors are used to simultaneously detect vertical and horizontal polarized fluorescence. The ratio of the two signals could then be computed after each laser shot. This would better normalize the signal to any variation in excited-state number density, as well as doubling the speed of data collection.) The ratio error was determined using the standard deviations found for each of the two data sets produced by 300 laser shots. The magnetic field was generated by a pair of Helmholtz coils surrounding the cesium cell. The field was measured to an accuracy of 1% using a Hall effect Gaussmeter.

B. Data analysis

A sample measured decoupling curve is shown in Fig. 7. The data were not corrected for the finite solid angle of the light detection system since this was small and did not affect the magnetic field half-width of the decoupling signal. A Lorentzian function was fit to the data using a least-squares algorithm that varied the half-width to obtain the optimum fit. The initial excited-state electronic density matrix was assumed to be given by the following:

$$\rho_e(0)=\frac{1}{2(1+\alpha)}(\alpha|3/2\rangle\langle 3/2|+|1/2\rangle\langle 1/2|+|-1/2\rangle\langle -1/2|+\alpha|-3/2\rangle\langle -3/2|)\ . \tag{19}$$

The parameter α is zero for the case of a two-photon excitation from an $S_{1/2}$ to a $D_{3/2}$ state generated by a laser linearly polarized along the quantization axis. The theoretical zero field decoupling curve value $R(0)$ is found using (15) and (16) to be 1.37 and agrees well with the experimental result. The observed high field value, however, is substantially lower than the predicted value of 4.0. The ratio $R(B)$ measures the amount of vertical polarized fluorescence produced by $\Delta m_J=0$ transitions relative to the amount of horizontal polarized fluorescence produced by $\Delta m_J=\pm 1$ transitions. Hence the observation that the ratio is lower than prediced means there are more $\Delta m_J=\pm 1$ decays than expected. This could happen if the $m_J=\pm 3/2$ sublevels of the $8D_{3/2}$ state are somehow initially populated. Several mechanisms that could do this will now be discussed.

The $\pm 3/2$ Zeman sublevels can be populated directly from the ground state if the laser linewidth is less than the hyperfine splitting of the ground state. Such an excitation generates an initial state having nuclear as well as electronic polarization. The ground-state hyperfine splitting was studied by scanning the laser wavelength across the two-photon absorption resonance, while monitoring the fluorescence produced by the $8D_{3/2}\rightarrow 6P_{1/2}$ transition. Two partially resolved peaks corresponding to the $F=3$ and 4 hyperfine levels of the ground state were observed. No measurable difference in field half-width was observed when the laser wavelength was tuned to either of these two peaks. The data shown in Fig. 7 were taken with the laser wavelength tuned to maximize the fluorescence signal.

The $\pm 3/2$ Zeeman sublevels can also be populated by collisions which transfer atoms from the $\pm 1/2$ sublevels of the excited state. However, at the cell temperature of 100 °C, the cesium number density[10] is only 10^{13} cm^{-3} and the mean time between collisions greatly exceeds the $\approx$150-nsec radiative lifetime of the $8D_{3/2}$ state.

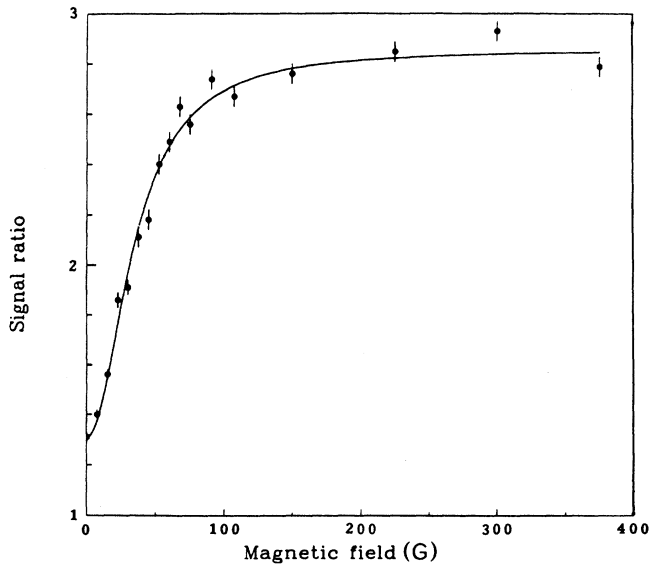

FIG. 7. Sample of experimental data: A Lorentzian function was fit to the data using a least-squares program that varied the field half-width $B_{1/2}$ to find the optimum fit.

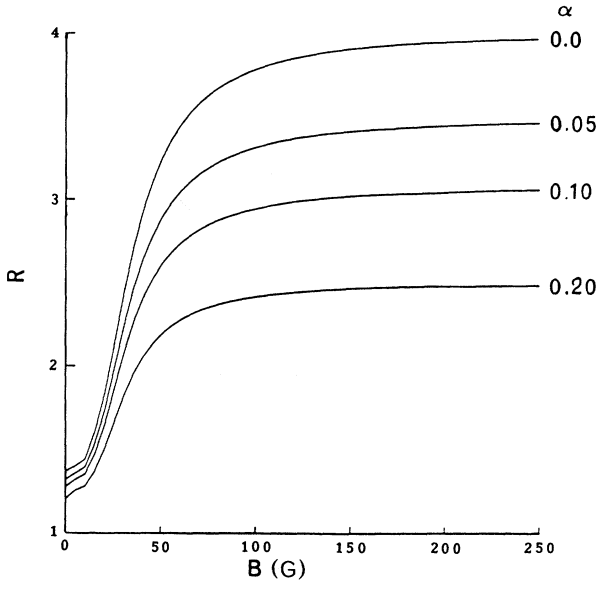

FIG. 8. Effect of initial state on signal ratio: The decoupling signal was computed for the state described by (19). The parameter α measures the fraction of atoms initially excited into the $\pm 3/2$ sublevels of a $D_{3/2}$ state. The $D_{3/2}$ state was specified to have a magnetic dipole constant $a=4.0$ MHz and to radiatively decay to a $P_{1/2}$ state.

Immediately after the two-photon excitation of the ground state, a population inversion exists between the $8D_{3/2}$ state and lower excited states. This can result in lasing action. An atom in the $\pm 1/2$ sublevel can be stimulated to emit a photon. Subsequently, it may absorb a photon and populate the $\pm 3/2$ sublevels of the $8D_{3/2}$ state. This process should be most significant at high laser pulse energies which create the largest population inversion. The stimulated emission cross section σ_{ef} can be estimated using the dipole sum rule

$$\int_0^\infty \sigma_{ef}(\nu)d\nu = \pi r_e c f_{fe} \frac{[J_f]}{[J_e]} \tag{20}$$

where r_e is the classical electron radius, c is the speed light, and f_{fe} is the absorption oscillator strength for the transition $f \rightarrow e$. Assuming a Lorentzian line shape, one finds the stimulated emission cross section at the transition frequency to be given by

$$\sigma_{ef} = \frac{4\pi r_e c f_{fe}}{\Gamma} \frac{[J_f]}{[J_e]} \tag{21}$$

where Γ is the transition linewidth. For the $8D_{3/2} \rightarrow 9P_{1/2}$ transition, a Coulomb-approximation calculation[11] has found $f_{fe}=0.64$ and $\Gamma = 10$ MHz.[12] The stimulated emission cross section then equals 3×10^{-9} cm^2. Unfortunately, direct observation of these lasing transitions was not possible since their wavelengths (≈ 57 μm) exceed the transmission limit of the Pyrex cell wall.

In this experiment, decoupling curves were generated using laser pulse energies between 1 and 10 mJ. The high field value of R was approximately 3 for laser energies of 1 mJ but was 2 at laser energies of 10 mJ. This behavior is compatible with the lasing hypothesis and agrees with observations that have been made using rubidium.[13] We wish to emphasize, however, that no dependence of the decoupling curve magnetic field half-width on the laser pulse energy was observed. The data shown in Fig. 7 were taken using an average laser pulse energy of 3.5 mJ.

The decoupling curves resulting from the density matrix described in (19) were computed and are shown in Fig. 8. The signal amplitude decreases rapidly as α increases. The signal reduces to zero when all the sublevels are equally populated. (i.e., $\alpha = 1$) The field half-width changes slowly with increasing α as is shown in Fig. 9. Hence the decoupling experiment is relatively insensitive to the precise composition of the initial state. Therefore α was set to zero when analyzing the data. The field half-width of the fitted Lorentzian function shown in Fig. 7, corrected for the vertical component of the earth's field, is 34.8 ± 1.0 G. The quoted error is due to the uncertainty with which the ratio could be determined at high fields due to scatter of the data, and to approximating the field half-width by the HWHM of the fitted Lorentzian function. The magnitude of the magnetic dipole hyperfine constant of the cesium $8D_{3/2}$ state was determined to be 3.92 ± 0.10 MHz using Fig. 5.

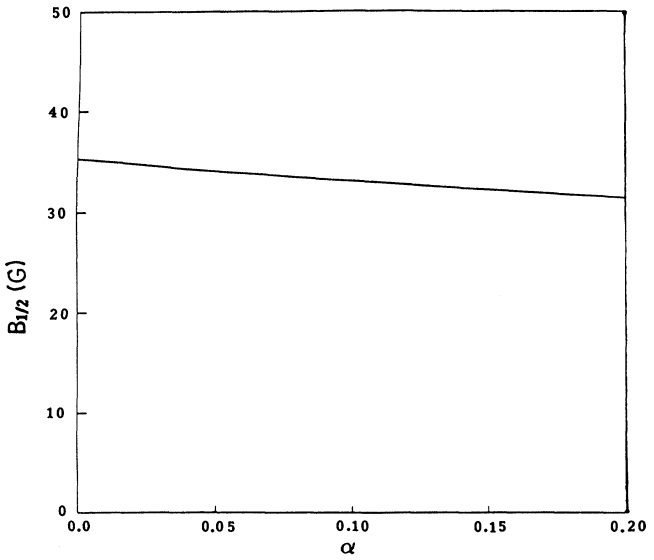

FIG. 9. Effect of initial state on magnetic-field half-width: The magnetic-field half-widths $B_{1/2}$ of the decoupling curves shown in Fig. 8 were determined and plotted vs α.

IV. CONCLUSION

This result agrees well with the values of 3.92 ± 0.07 MHz obtained by a quantum-beats experiment[14] and 3.98 ± 0.12 MHz found using level-crossing spectroscopy.[1] Both experiments assumed the cesium electric quadrupole moment to be negligible. The advantage of this decoupling experiment is its simplicity. The Zeeman sublevels of the excited state must initially be populated anisotropically. This is readily done using a polarized laser to excite an unpolarized atom. Fluorescence resulting from the decay of the excited state is detected by a photomultiplier and integrated by a boxcar integrator. Fast and relatively expensive transient digitizers required by quantum-beats experiments are not needed. Finally, the data analysis is much easier than that for a level-crossing experiment, since the decoupling curve is very well approximated by a Lorentzian function, rather than a complicated numerically computed signal.

In this experiment, the magnetic dipole constant was determined from the plot of a ratio of two integrated fluorescent intensities versus the magnetic field. For many states, this decoupling curve does not depend on the state lifetime. Moreover, the signal ratio is independent of the excited-state number density which is difficult to determine. This is of special importance for a state populated by multiphoton absorption from the ground state since any shot to shot fluctuation of the laser energy can cause substantial variation of the excited-state population. Finally, we wish to emphasize that the magnetic dipole constant is determined by the half-width rather than the amplitude of a Lorentzian signal. Hence, it is

relatively insensitive to the precise composition of the initial state or to atomic collisions that strongly change the signal amplitude. Hence, we conclude that the decoupling method is simple and useful for measuring hyperfine structure especially of states accessible using multiphoton excitation of the ground state.

ACKNOWLEDGMENTS

This work was supported by the Canadian National Science and Engineering Research Council and by York University. The authors are grateful to Will Happer for the use of a cesium cell.

[1]S. Svanberg, P. Tsekeris, and W. Happer, Phys. Rev. Lett. **30**, 817 (1973).

[2]W. A. van Wijngaarden, K. D. Bonin, and W. Happer, Phys. Rev. A **33**, 77 (1986).

[3]E. Arimondo, M. Inguscio, and P. Violino, Rev. Mod. Phys. **49**, 31 (1977).

[4]P. Buck, I. I. Rabi, and B. Senitzky, Phys. Rev. **86**, 308 (1952).

[5]A. Corney, *Atomic and Laser Spectroscopy* (Clarendon, Oxford, 1977).

[6]Oriented atoms are useful for determining the sign of the hyperfine coupling constants, as is discussed in C. Tai, W. Happer, and R. Gupta, Phys. Rev. A **12**, 736 (1975).

[7]U. Fano, Rev. Mod. Phys. **29**, 74 (1957).

[8]K. Blum, *Density Matrix Theory and Applications* (Plenum, New York, 1981).

[9]R. Gupta, S. Chang, and W. Happer, Phys. Rev. A **6**, 529 (1972).

[10]A. N. Nesmeianov, *Vapor Pressure of The Elements* (Academic, New York, 1963).

[11]D. R. Bates and A. Damgaard, Philos. Trans. R. Soc. London **242**, 101 (1949).

[12]P. Tsekeris (private communication).

[13]W. A. van Wijngaarden, Ph.D. thesis, Princeton University, 1986 (unpublished).

[14]J. S. Deech, R. Luypaert, and G. W. Series, J. Phys. B **8**, 1406 (1975).